Matrix Isolation Infrared Spectroscopic and Theoretical Study of Noble Gas Coordinated Rhodium−Dioxygen Complexes

Rui Yang, Yu Gong, Han Zhou, and Mingfei Zhou*

Department of Chemistry & Laser Chemistry Institute, Shanghai Key Laboratory of Molecular Catalysts and Innovative Materials, Fudan University, Shanghai 200433, People's Republic of China

Received: September 21, 2006; In Final Form: October 30, 2006

Reactions of rhodium atoms with dioxygen molecules in solid argon have been investigated using matrix isolation infrared absorption spectroscopy. The rhodium−dioxygen complexes, Rh(η^2-O_2), Rh(η^2-O_2)$_2$, and Rh(η^2-O_2)^2(η^1-OO), are produced spontaneously on annealing. The Rh(η^2-O_2) complex rearranges to the inserted RhO_2 molecule under visible light irradiation. Experiments doped with xenon in argon show that the rhodium−dioxygen complexes are coordinated by one or two noble gas atoms in solid noble gas matrixes. Hence, the Rh(η^2-O_2), Rh(η^2-O_2)$_2$, and Rh(η^2-O_2)$_2$(η^1-OO) molecules trapped in solid noble gas matrixes should be regarded as the Rh(η^2-O_2)(Ng)$_2$, Rh(η^2-O_2)$_2$(Ng)$_2$, and Rh(η^2-O_2)$_2$(η^1-OO)(Ng) (Ng = Ar or Xe) complexes. The product absorptions are identified on the basis of isotopic substitution and density functional theory calculations.

Introduction

Transition metal oxides are widely used as catalysts and catalytic supports in many important chemical processes. The investigation of the electronic and geometric structures and reactivities of simple transition metal oxides is important in understanding the nature of active species in catalysis at the molecular level. Rhodium−dioxygen complexes have been shown to be important reactive intermediates in many rhodium-mediated oxidation reactions.[1] The rhodium monoxide molecule has been well studied.[2−4] Its ground state as well as several excited states were investigated in the gas phase.[2,3] Spectroscopic studies on rhodium−dioxygen complexes as well as rhodium dioxide molecules have also been reported.[5−8] A number of mono-, di-, and trinuclear rhodium−dioxygen complexes were produced by the reactions of thermally generated rhodium atoms and small clusters with dioxygen in noble gas matrixes and were characterized using the infrared and UV−visible absorption spectroscopies.[5,6] The rhodium dioxide molecule has been produced by the reaction of laser-vaporated rhodium atoms with dioxygen in solid argon.[7,8] The RhO_2 molecule was established by electron spin resonance spectra to have a $^2\Sigma_g$ ground state with a linear structure. However, rhodium−dioxygen complexes were not observed.[7] Recently, the reaction products from laser-ablated rhodium atoms and dioxygen have also been investigated using infrared absorption spectroscopy. A number of rhodium oxides and dioxygen complex absorptions were observed. The experimental observations suggest that some of the previous dioxygen complex assignments are incorrect, but definitive identification of these complexes was not made.[8] Hence, a study of the reactions of rhodium atoms and dioxygen in solid argon was carried out. The resulting mononuclear rhodium−dioxygen complexes were identified via different O_2 concentration and laser energy experiments together with detailed isotopic substitution and density functional theory (DFT) calculations. In addition, the experiments doped with xenon in argon provide new evidence that these rhodium dioxygen complexes are coordinated by one or two noble gas atoms in solid argon matrix.

Experimental and Computational Methods

The experimental setup for pulsed laser-evaporation and matrix isolation infrared spectroscopic investigation has been described in detail previously.[9] Briefly, the 1064 nm fundamental of a Nd:YAG laser (Continuum, Minilite II, 10 Hz repetition rate and 6 ns pulse width) was focused onto a rotating rhodium metal target (Johnson Matthey, 99.9%) through a hole in a CsI window cooled normally to 6 K by means of a closed-cycle helium refrigerator (ARS, 202N). The laser-evaporated metal atoms were co-deposited with oxygen and noble gas mixtures onto the CsI window. In general, matrix samples were deposited for 1−2 h at a rate of 4 mmol/h. The O_2/Ar and O_2/Xe/Ar mixtures were prepared in a stainless steel vacuum line using the standard manometric technique. Isotopic $^{18}O_2$ (ISOTEC, 99%) was used without further purification. The infrared absorption spectra of the resulting sample were recorded on a Bruker IFS 66V spectrometer at 0.5 cm^{-1} resolution between 4000 and 400 cm^{-1} using a liquid nitrogen cooled HgCdTe (MCT) detector. Samples were annealed at different temperatures and subjected to broadband irradiation using a tungsten lamp or a high-pressure mercury arc lamp with glass filters.

Quantum chemical calculations were performed using the Gaussian 03 program.[10] The three-parameter hybrid functional according to Becke with additional correlation corrections due to Lee, Yang, and Parr (B3LYP)[11,12] was utilized. The aug-cc-PVTZ basis set was used for the O and Ar atoms, and the SDD pseudo potential and basis set was used for the Rh and Xe atoms.[13,14] The geometries were fully optimized; the harmonic vibrational frequencies were calculated, and zero-point vibrational energies (ZPVE) were derived.

* Corresponding author. E-mail: mfzhou@fudan.edu.cn.

10.1021/jp0662000 CCC: $37.00
Published on Web 12/13/2006

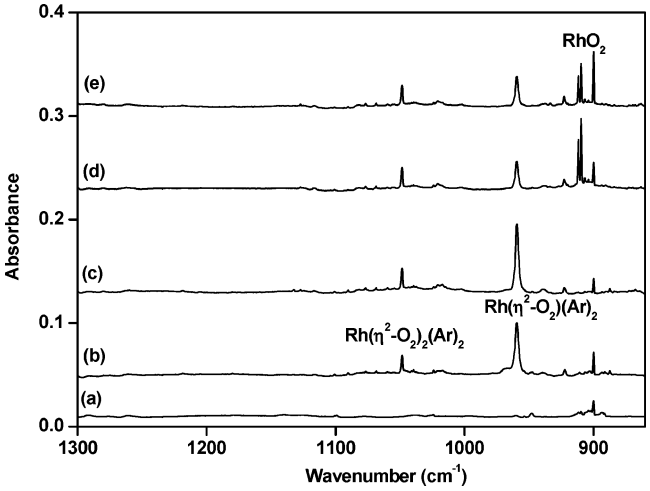

Figure 1. Infrared spectra in the 1300−860 cm^{-1} region from co-deposition of laser-evaporated rhodium atoms with 0.05% O_2 in argon. (a) 1 h of sample deposition at 6 K, (b) after 25 K annealing, (c) after 35 K annealing, (d) after 15 min of $\lambda > 500$ nm irradiation, and (e) after 35 K annealing.

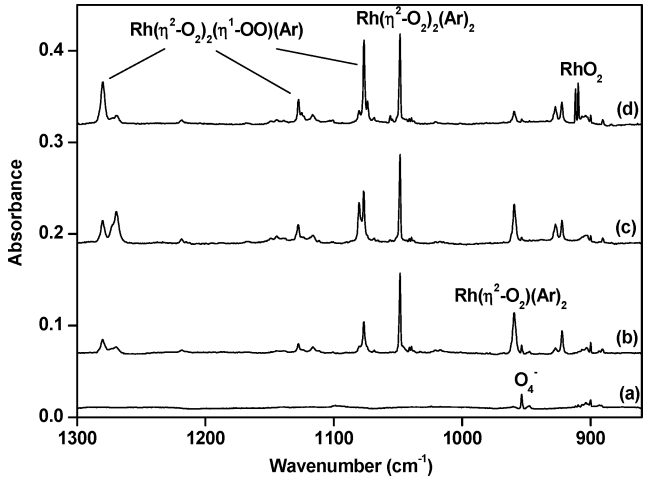

Figure 2. Infrared spectra in the 1300−860 cm^{-1} region from co-deposition of laser-evaporated rhodium atoms with 0.2% O_2 in argon. (a) 1 h of sample deposition at 6 K, (b) after 25 K annealing, (c) after 35 K annealing, and (d) after 15 min of $\lambda > 500$ nm irradiation.

Results and Discussion

Infrared Spectra. A series of experiments were performed using different O_2 concentrations (ranging from 0.02% to 0.5% in argon) and different laser energies to control the relative concentrations of Rh and O_2. The infrared spectra in selected regions with 0.05% O_2 in argon with 10 mJ/pulse laser energy are illustrated in Figure 1. Only a very weak absorption at 899.9 cm^{-1} was observed after sample deposition at 6 K (trace a). Two new absorptions at 959.5 and 1048.4 cm^{-1} were produced on sample annealing to 25 K (trace b). The 1048.4 cm^{-1} absorption increased on sample annealing to 35 K (trace c) and remained almost unchanged on broadband ($500 < \lambda < 1000$ nm) irradiation (trace d). The 959.5 cm^{-1} absorption also increased on sample annealing to 35 K, but markedly decreased upon $\lambda > 500$ nm irradiation, during which two absorptions at 911.7 and 909.6 cm^{-1} were produced. The 911.7 and 909.6 cm^{-1} absorptions decreased upon subsequent sample annealing to 35 K (trace e), while the 899.9 cm^{-1} absorption was greatly enhanced. A weak band at 562.4 cm^{-1} (not shown), which was previously assigned to the cyclic-Rh_2O_2 molecule, appeared and increased on annealing and disappeared on broadband irradiation.[8]

Figure 2 shows the spectra with 0.2% O_2 in argon using the same laser energy as the experiment shown in Figure 1. The O_4^- anion absorption was observed at 953.8 cm^{-1} on sample deposition (trace a).[15] The 959.5 cm^{-1} absorption appeared on 25 K annealing, decreased on 30 K annealing, and almost disappeared under $\lambda > 500$ nm irradiation. The 1048.4 cm^{-1} absorption also was produced on 25 K annealing, and remained unchanged upon high temperature (30 K) annealing and broadband irradiation. Three new absorptions at 1076.7, 1127.6, and 1280.1 cm^{-1}, which were not observed in the experiment with low O_2 concentration (Figure 1), appeared on sample annealing to 25 K, and markedly increased on high temperature annealing. Both the 1280.1 and the 1076.7 cm^{-1} absorptions have one site absorption at 1269.3 and 1080.4 cm^{-1}, which increased on annealing but were converted to the 1280.1 and 1076.7 cm^{-1} absorption sites under $\lambda > 500$ nm irradiation. The cyclic-Rh_2O_2 absorption at 562.4 cm^{-1} was not observed in this experiment. It is noteworthy that the RhO and O_3 absorptions were barely observed in both the low and the high O_2 concentration experiments by using relatively low laser energy.[8]

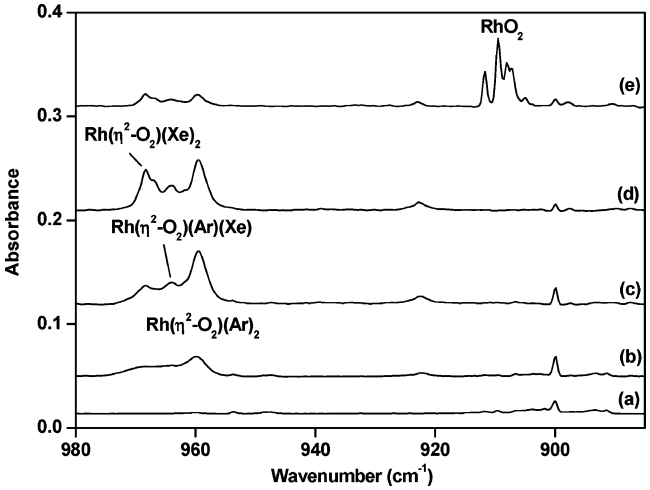

Figure 3. Infrared spectra in the 980−885 cm^{-1} region from co-deposition of laser-evaporated rhodium atoms with 0.05% O_2 + 0.2% Xe in argon. (a) 1 h of sample deposition at 6 K, (b) after 20 K annealing, (c) after 30 K annealing, (d) after 40 K annealing, and (e) after 15 min of $\lambda > 250$ nm irradiation.

Recent investigations showed that some transition and actinide metal oxide species trapped in solid noble gas matrixes are coordinated by multiple noble gas atoms in forming noble gas complexes.[16−22] To determine whether the product molecules trapped in solid argon are coordinated by noble gas atoms or not, and to determine the number of noble gas atoms that bind intimately to the product molecules in the first coordination sphere, experiments were performed by using mixtures of argon doped with xenon. Figure 3 shows the spectra in the 980−885 cm^{-1} region from co-deposition of laser-evaporated rhodium atoms with 0.05% O_2 doped with 0.2% Xe in argon. Besides the 959.5 cm^{-1} absorption, two new absorptions at 964.0 and 968.4 cm^{-1} were produced on sample annealing to different temperatures (traces b−d). These absorptions decreased on $\lambda > 500$ nm irradiation and produced the 911.7 and 909.6 cm^{-1} absorptions with a broad shoulder at the low-frequency side of the 909.6 cm^{-1} absorption (trace e). The spectra in the 1300−980 cm^{-1} region from co-deposition of laser-evaporated rhodium

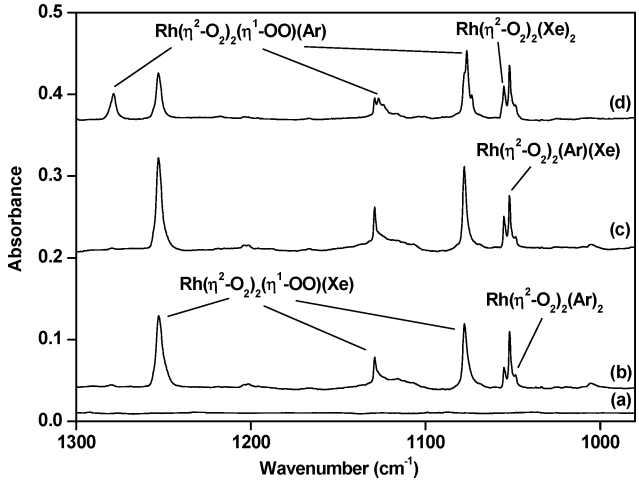

Figure 4. Infrared spectra in the 1300−980 cm^{-1} region from co-deposition of laser-evaporated rhodium atoms with 0.2% O_2 + 1% Xe in argon. (a) 1 h of sample deposition at 6 K, (b) after 35 K annealing, (c) after after 43 K annealing, and (d) after 15 min of $\lambda > 500$ nm irradiation.

atoms with 0.2% O_2 doped with 1% Xe in argon are illustrated in Figure 4. The 1048.4 cm^{-1} absorption is very weak, and new absorptions at 1252.9, 1129.2, 1077.8, 1055.1, and 1051.8 cm^{-1} were produced on sample annealing (traces b and c). The 1252.9, 1129.2, and 1077.8 cm^{-1} absorptions decreased on $\lambda > 500$ nm irradiation and produced the absorptions at 1278.7, 1126.9, and 1076.4 cm^{-1} (trace d). All of the product absorptions are listed in Table 1.

Isotopic substitution was employed for characterization of absorptions, and the results are also listed in Table 1. Similar spectra were observed using $^{18}O_2$, and all of the product absorptions exhibited isotopic shifts. Experiments with mixed $^{16}O_2$ + $^{18}O_2$ and $^{16}O_2$ + $^{16}O^{18}O$ + $^{18}O_2$ were also done. The spectra in selected regions using different isotopic O_2 samples are shown in Figures 5 and 6, respectively.

RhO_2. The 899.9 cm^{-1} absorption was assigned previously to the antisymmetric ORhO stretching mode of the inserted RhO_2 molecule.[8] As shown in Figure 1, the 899.9 cm^{-1} absorption increased at the expense of the 909.6 and 911.7 cm^{-1} absorptions. The isotopic shifts (Table 1) and splittings (Figure 5) indicate that the 909.6 and 911.7 cm^{-1} absorptions are also due to antisymmetric ORhO stretching vibration, and only two equivalent O atoms are involved. We assign the 909.6 and 911.7 cm^{-1} absorptions to RhO_2 at different trapping sites. In the xenon doping experiment, no distinct new absorptions were produced, suggesting that the RhO_2 molecule is not coordinated by argon atoms in solid argon. DFT calculations predicted that the RhO_2 molecule has a $^2A_1$ ground state with a near linear structure (bond angle of 155.7°), in agreement with previous calculations.[8] The antisymmetric ORhO stretching mode was predicted at 974.6 cm^{-1}. Calculations also found that RhO_2 is not able to coordinate argon atoms (geometry optimization on $ArRhO_2$ almost converged to RhO_2 + Ar), which is consistent with the experimental observations.

Rh(η^2-O_2)$_2$(Ng)$_2$ (Ng = Ar, Xe). The 959.5 cm^{-1} absorption shifted to 907.9 cm^{-1}, giving an isotopic $^{16}O/^{18}O$ ratio of 1.0568, which suggests that it is due to an O−O stretching vibration. The isotopic splittings in the mixed $^{16}O_2$ + $^{18}O_2$ and $^{16}O_2$ + $^{16}O^{18}O$ + $^{18}O_2$ experiments (Figure 5) clearly show that one O_2 unit with two equivalent O atoms is involved in this mode. The 959.5 cm^{-1} band is a major product absorption in all of the experiments. As can be seen in Figure 1, the absorptions at 911.7/909.6 cm^{-1} due to the inserted RhO_2 molecule were produced at the expense of the 959.5 cm^{-1} absorption upon $\lambda > 500$ nm irradiation. These experimental observations suggest that only one rhodium atom is likely involved in the 959.5 cm^{-1} absorption. Therefore, the 959.5 cm^{-1} absorption involves a Rh-(η^2-O_2) unit. The experiment with xenon doped in argon shown in Figure 3 demonstrates that two new absorptions at 964.0 and 968.4 cm^{-1} were produced on annealing at the expense of the 959.5 cm^{-1} absorption. The 964.0 and 968.4 cm^{-1} absorptions exhibit about the same isotopic $^{16}O/^{18}O$ ratios as the 959.5 cm^{-1} absorption. These observations suggest that the 959.5 cm^{-1} absorption species also involves two argon atoms. Accordingly, the 959.5 cm^{-1} absorption is assigned to the O−O stretching mode of the Rh(η^2-O_2)(Ar)$_2$ complex isolated in solid argon, and the 964.0 and 968.4 cm^{-1} absorptions produced in Xe-doped experiments are due to the Rh(η^2-O_2)(Ar)(Xe) and Rh(η^2-O_2)-(Xe)$_2$ complexes resulting from the successive replacement of coordinated Ar atoms by Xe atoms.

Quantum chemical calculations were performed to support the assignment. DFT/B3LYP calculations were performed on the doublet and quartet spin states of Rh(η^2-O_2), and the results are summarized in Table 2 and Figure 7. An $^2A_2$ state is found to be the ground state of Rh(η^2-O_2), in agreement with the previous calculations.[8] The lowest quartet state with a C_{2v} symmetry is a transition state with one imaginary frequency, while a $^4A''$ state with O_2 end-on bonded is predicted to be stable and lies only 2.7 kcal/mol higher in energy than the $^2A_2$ state. The calculation results also indicate that the $^2A_2$ state of Rh(η^2-O_2) can coordinate two Ar or Xe atoms in forming the noble gas complexes. As shown in Figure 7, the Rh(η^2-O_2)-(Ng)$_2$ (Ng = Ar, Xe) complexes were predicted to have an $^2A_2$ ground state with a planar C_{2v} structure. The calculated O−O stretching frequencies of the Rh(η^2-O_2)(Ar)$_{2-x}$(Xe)$_x$ (x = 0, 1, 2) series exhibit the monotonic blue-shift upon successively replacement of Ar atoms by Xe atoms (Table 3). The calculated blue-shifts of the O−O stretching mode for successively substituting Ar atoms by Xe atoms are 3.5 and 7.7 cm^{-1}, respectively, which are in excellent agreement with the experimentally determined shifts of 4.5 and 8.9 cm^{-1}.

In an earlier matrix isolation infrared study of reaction of thermal evaporated rhodium atoms and dioxygen, a band at 908 cm^{-1} was assigned to the Rh(η^2-O_2) molecule.[5] The 908 cm^{-1} absorption corresponds to the 909.6 cm^{-1} absorption in the present study. As is already being pointed out,[8] this absorption exhibits an isotopic $^{16}O/^{18}O$ ratio that is characteristic of the antisymmetric ORhO stretching vibration of the ORhO molecule. In a more recent investigation, a weak band at 1090.2 cm^{-1} was tentatively assigned to Rh(η^2-O_2).[8] No absorption around the 1090 cm^{-1} region was observed in the present study at all experimental conditions.

Rh(η^2-O_2)$_2$(Ng)$_2$ (Ng = Ar, Xe). The 1048.4 cm^{-1} absorption was previously assigned to the Rh(η^2-O_2)$_2$ complex.[5,8] Our experimental observations also agree that the molecule involves two equivalent O_2 subunits with four equivalent O atoms. As shown in Figure 5, besides the antisymmetric O−O stretching frequencies of Rh(η^2-$^{16}O_2$)$_2$, Rh(η^2-$^{16}O_2$)(η^2-$^{18}O_2$), and Rh(η^2-$^{18}O_2$)$_2$, a weak absorption at 1076.7 cm^{-1} was also observed. This band is due to the symmetric O−O stretching mode of the Rh(η^2-$^{16}O_2$)(η^2-$^{18}O_2$) molecule. In addition, two new absorptions at 1051.8 and 1055.1 cm^{-1} were produced when xenon was doped into the argon matrix (Figure 4), and these new absorptions increased on annealing after the 1048.4 cm^{-1} absorption. The 1051.8 and 1055.1 cm^{-1} bands shifted to 993.5 and 996.7 cm^{-1} with the $^{18}O_2$ sample, and gave the $^{16}O/^{18}O$ isotopic frequency ratios the same as that of the 1048.4 cm^{-1}

TABLE 1: Infrared Absorptions (cm^{-1}) from the Reactions of Laser-Evaporated Rhodium Atoms with Dioxygen in Solid Argon

$^{16}O_2$	$^{18}O_2$	$^{16}O_2 + {}^{18}O_2$	$^{16}O_2 + {}^{16}O^{18}O + {}^{18}O_2$	assignment
1280.1	1207.6	1279.4, 1208.4	1279.6, 1244.8, 1208.3	Rh(η^2-O$_2$)$_2$(η^1-OO)(Ar)
1269.3	1198.1	1268.6, 1198.6	1268.8, 1235.4, 1198.4	Rh(η^2-O$_2$)$_2$(η^1-OO)(Ar) site
1127.6	1064.6	1126.7, 1120.7, 1064.6		Rh(η^2-O$_2$)$_2$(η^1-OO)(Ar)
1076.7	1016.4	1076.5, 1044.3, 1016.6		Rh(η^2-O$_2$)$_2$(η^1-OO)(Ar)
1080.4	1019.8	1080.1, 1044.6, 1019.9		Rh(η^2-O$_2$)$_2$(η^1-OO)(Ar) site
1252.9	1182.5			Rh(η^2-O$_2$)$_2$(η^1-OO)(Xe)
1129.2	1066.1			Rh(η^2-O$_2$)$_2$(η^1-OO)(Xe)
1077.8	1016.6			Rh(η^2-O$_2$)$_2$(η^1-OO)(Xe)
1048.4	990.3	1076.7, 1048.4, 1002.8, 990.3	1048.4, 1028.9, 1019.4, 1002.8, 999.8, 990.3	Rh(η^2-O$_2$)$_2$(Ar)$_2$
1051.8	993.5			Rh(η^2-O$_2$)$_2$(Ar)(Xe)
1055.1	996.7			Rh(η^2-O$_2$)$_2$(Xe)$_2$
959.5	907.9	959.5, 907.9	959.5, 934.4, 907.9	Rh(η^2-O$_2$)(Ar)$_2$
964.0	911.2			Rh(η^2-O$_2$)(Ar)(Xe)
968.4	916.8			Rh(η^2-O$_2$)(Xe)$_2$
911.7	872.3	911.7, 872.3	911.7, 899.9, 872.3, 831.2	RhO$_2$ site
909.6	870.2	909.6, 870.2	909.6, 897.8, 870.2, 829.4	RhO$_2$ site
899.9	861.1	899.9, 861.1	899.9, 888.0, 861.1	RhO$_2$

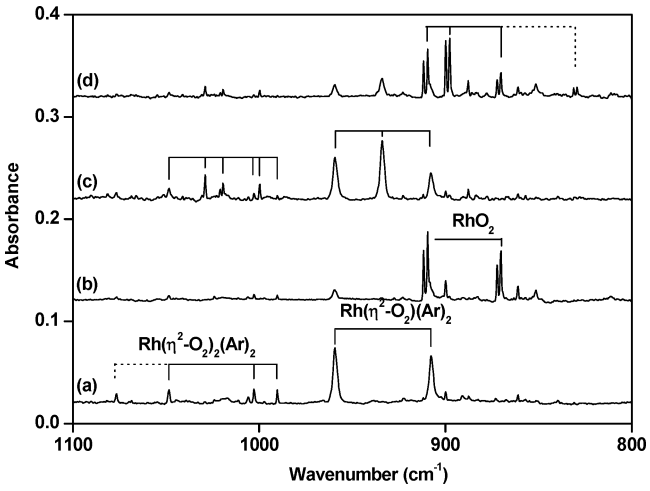

Figure 5. Infrared spectra in the 1100−800 cm^{-1} region from co-deposition of laser-evaporated rhodium atoms with isotopic-labeled samples in excess argon. (a) 0.025% $^{16}O_2$ + 0.025% $^{18}O_2$, 2 h of sample deposition followed by 30 K annealing, (b) after 15 min of λ > 500 nm irradiation of sample (a), (c) 0.025% $^{16}O_2$ + 0.05% $^{16}O^{18}O$ + 0.025% $^{18}O_2$, 2 h of sample deposition followed by 30 K annealing, and (d) after 15 min λ > 500 nm irradiation of sample (c).

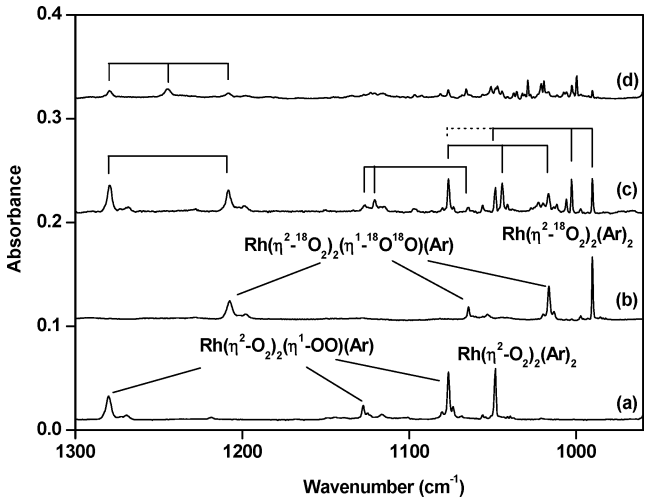

Figure 6. Infrared spectra in the 1300−960 cm^{-1} region from co-deposition of laser-evaporated rhodium atoms with isotopic-labeled samples in excess argon. Spectra were taken after 2 h of sample deposition followed by 15 min λ > 500 nm irradiation. (a) 0.2% $^{16}O_2$, (b) 0.2% $^{18}O_2$, (c) 0.1% $^{16}O_2$ + 0.1% $^{18}O_2$, and (d) 0.05% $^{16}O_2$ + 0.1% $^{16}O^{18}O$ + 0.05% $^{18}O_2$.

absorption. These experimental observations indicate that the 1048.4 cm^{-1} absorption should be assigned to the Rh(η^2-O$_2$)$_2$-(Ar)$_2$ complex instead of Rh(η^2-O$_2$)$_2$, and the 1051.8 and 1055.1 cm^{-1} absorptions in Xe-doped experiments are due to the Rh-(η^2-O$_2$)$_2$(Ar)(Xe) and Rh(η^2-O$_2$)$_2$(Xe)$_2$ complexes isolated in solid argon.

Theoretical calculations lend strong support to the above assignment. The Rh(η^2-O$_2$)$_2$ molecule was predicted to have a $^4B_{1u}$ ground state with a planar D_{2h} symmetry (Figure 7). In addition, B3LYP calculations predicted that Rh(η^2-O$_2$)$_2$ can coordinate two Ar or Xe atoms in forming the Rh(η^2-O$_2$)$_2$(Ng)$_2$ complexes, which were predicted to have a D_{2h} symmetry with the two noble gas atoms lying perpendicular to the RhO$_4$ plane. The Rh−Ng interactions are very weak with quite long Rh−Ng bond distances. The antisymmetric O−O stretching mode of Rh(η^2-O$_2$)$_2$(Ar)$_2$ was predicted to be 1178.8 cm^{-1}, ca. 95.4 cm^{-1} above the O−O stretching mode of the Rh(η^2-O$_2$)(Ar)$_2$ complex calculated at the same level of theory, which is in accord with the observed difference of 88.9 cm^{-1}. The O−O stretching frequency blue-shifted by 2.4 cm^{-1} when the two coordinated Ar atoms were replaced by two Xe atoms, which is smaller than the observed shift of 6.3 cm^{-1}. The calculations slightly underestimate the Rh−Ng bonding because of the lack of proper treatment for dispersive interactions with B3LYP.[23]

Rh(η^2-O$_2$)$_2$(η^1-OO)(Ng) (Ng = Ar, Xe). The absorptions at 1280.1, 1127.6, and 1076.7 cm^{-1} were observed in the previous experiments, which were attributed to dirhodium species.[5,6,8] We disagree on the assignment of dirhodium species. These absorptions kept constant relative intensities throughout all of the experiments, indicating that they are due to different vibrational modes of the same species. As can be seen in Figures 1 and 2, these absorptions are favored with relatively high O_2 concentrations and increased on annealing after the Rh(η^2-O$_2$)$_2$-(Ar)$_2$ absorption. It is important to point out that at the

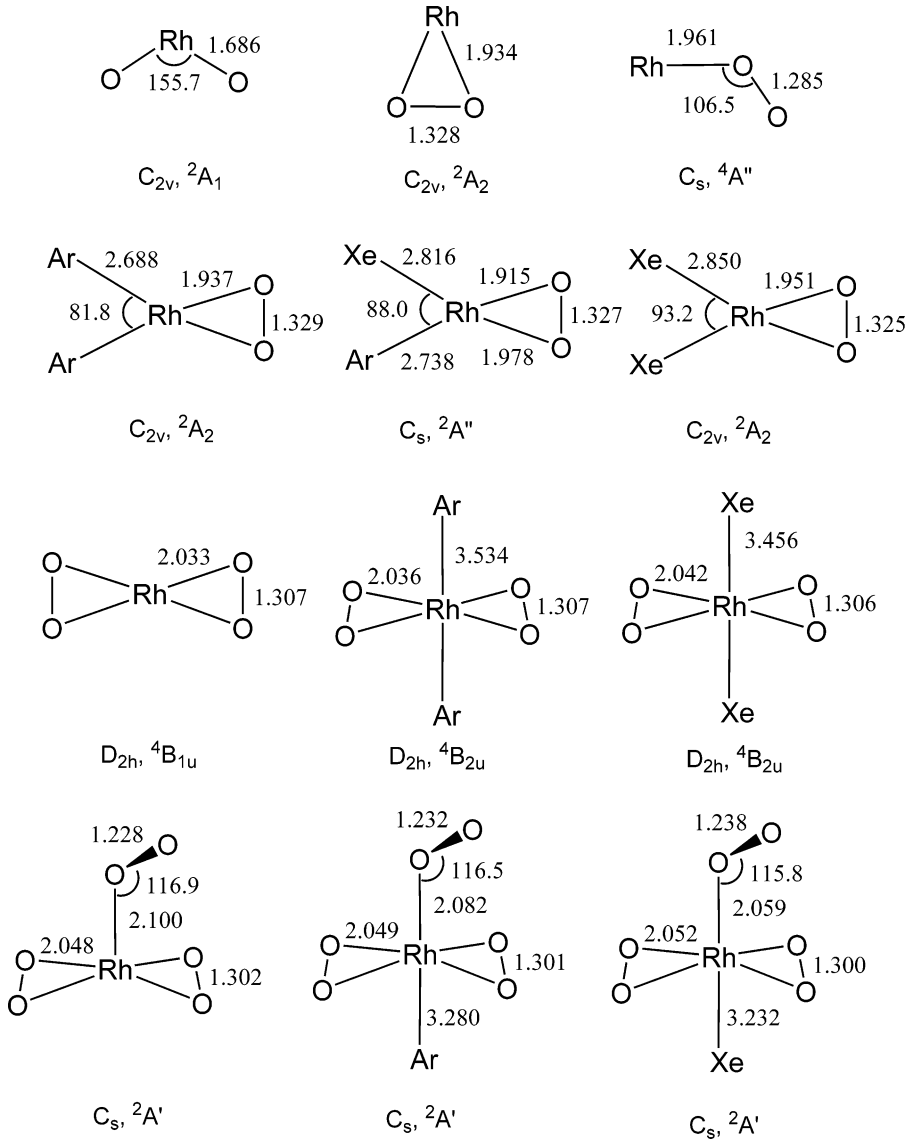

Figure 7. Optimized geometric parameters (bond lengths in angstrom and bond angles in deg) of the product molecules.

TABLE 2: Calculated Total Energies (in hartree after Zero-Point Energy Corrections), Vibrational Frequencies (cm^{-1}), and Intensities (km/mol) of the RhO_2 and $RhO_2(Ng)_2$ (Ng = Ar, Xe) Molecules

	energy	ν_1	ν_2	ν_3
RhO_2 ($^2A_1$)	−260.976976	942.0 (9)	169.2 (13)	974.6 (267)
Rh(η^2-O_2) ($^2A_2$)	−260.920510	1084.4 (194)	534.2 (1)	152.0 (17)
RhOO ($^4A''$)	−260.916180	1212.1 (295)	458.1 (4)	135.5 (3)
Rh(η^2-O_2)$(Ar)_2$ ($^2A_2$)	−1316.051112	1083.4 (270)	529.9 (6)	266.7 (5)
Rh(η^2-O_2)(Ar)(Xe) ($^2A''$)	−804.036714	1086.9 (325)	518.9 (13)	295.2 (6)
Rh(η^2-O_2)$(Xe)_2$ ($^2A_2$)	−292.021479	1091.1 (356)	499.4 (14)	250.8 (1)
Ar	−527.560002			
Xe	−15.539282			

experimental condition of Figure 2, which favors the formation of these three absorptions, the dirhodium species, cyclic-Rh_2O_2, was not formed. This suggests that the species most likely involves only one rhodium. The 1280.1 cm^{-1} absorption shifted to 1207.6 cm^{-1} with $^{18}O_2$. Both the band position and the isotopic $^{16}O/^{18}O$ ratio indicate that it is due to an O−O stretching vibration. In the mixed $^{16}O_2 + {}^{18}O_2$ experiment, the 1280.1 cm^{-1} absorption gave a broad doublet at 1279.4 and 1208.4 cm^{-1} with the $^{16}O_2$ and $^{18}O_2$ counterparts slightly shifted from the band positions in the pure $^{16}O_2$ or $^{18}O_2$ experiments. This clearly indicates that the 1280.1 cm^{-1} mode involves one O_2 subunit and is weakly coupled by other O_2 subunits. The 1127.6 and 1076.7 cm^{-1} absorptions also exhibit isotopic $^{16}O/^{18}O$ ratios that are indicative of O−O stretching vibrations. In the mixed $^{16}O_2 + {}^{18}O_2$ experiement, both absorptions split into a triplet (Figure 6), indicating that two equivalent O_2 subunits are involved in these two modes. The above experimental observations suggest the assignment of the 1280.1, 1127.6, and 1076.7 cm^{-1} absorptions to a $Rh(O_2)_3$ species involving three O_2 subunits with two of them being equivalent. When xenon atoms are doped into argon, a new group of absorptions at 1252.9, 1129.2, and 1077.8 cm^{-1} was produced (Figure 4), which suggests that the molecule involves one noble gas atom. Accordingly, we assign the 1280.1, 1127.6, and 1076.7 cm^{-1} absorptions to

TABLE 3: Calculated Total Energies (in hartree after Zero-Point Energy Corrections), O−O Stretching Frequencies (cm^{-1}), and Intensities (km/mol) of the Rh(η^2-O_2)$_2$ and Rh(η^2-O_2)$_2$(η^1-OO) Molecules and Their Noble Gas Complexes[a]

	state	total energy	calcd.	exp.
Rh(η^2-O_2)$_2$	$^4B_{1u}$	−411.358933	1223.7 (0)	
			1178.9 (314)	
Rh(η^2-O_2)$_2$(Ar)$_2$	$^4B_{2u}$	−1466.478870	1223.6 (0)	
			1178.8 (290)	1048.4
Rh(η^2-$^{16}O_2$)(η^2-$^{16}O^{18}O$)(Ar)$_2$			1212.1 (32)	
			1156.5 (250)	1028.9
Rh(η^2-$^{16}O_2$)(η^2-$^{18}O_2$)(Ar)$_2$			1207.5 (71)	1076.7
			1126.2 (203)	1002.8
Rh(η^2-$^{16}O^{18}O$)$_2$(Ar)$_2$			1189.1 (0)	
			1145.7 (274)	1019.4
Rh(η^2-$^{18}O_2$)(η^2-$^{16}O^{18}O$)(Ar)$_2$			1177.6 (33)	
			1122.3 (233)	999.8
Rh(η^2-$^{18}O_2$)$_2$(Ar)$_2$			1153.5 (0)	
			1111.4 (258)	990.3
Rh(η^2-O_2)$_2$(Xe)$_2$	$^4B_{2u}$	−442.439087	1226.0 (0)	
			1181.2 (259)	1055.1
Rh(η^2-O_2)$_2$(η^1-OO)	$^2A'$	−561.746494	1413.2 (338)	
			1238.0 (13)	
			1191.0 (282)	
Rh(η^2-O_2)$_2$(η^1-OO)(Ar)	$^2A'$	−1089.306628	1390.6 (414)	1280.1
			1240.5 (16)	1127.6
			1193.8 (271)	1076.7
Rh(η^2-$^{16}O_2$)$_2$(η^1-$^{18}O^{18}O$)(Ar)			1311.8 (353)	1208.4
			1239.6 (29)	1126.7
			1193.8 (271)	1076.5
Rh(η^2-O_2)(η^2-$^{18}O_2$)(η^1-OO)(Ar)			1390.4 (416)	1279.4
			1223.9 (76)	1120.7
			1140.8 (194)	1044.3
Rh(η^2-$^{18}O_2$)$_2$(η^1-OO)(Ar)			1390.3 (418)	1279.4
			1169.7 (11)	1064.6
			1125.4 (242)	1016.6
Rh(η^2-$^{18}O_2$)$_2$(η^1-$^{18}O^{18}O$)(Ar)			1310.9 (368)	1207.6
			1169.4 (14)	1064.6
			1125.4 (242)	1016.4
Rh(η^2-O_2)$_2$(η^1-OO)(Xe)	$^2A'$	−577.287471	1350.5 (578)	1252.9
			1243.9 (25)	1129.2
			1197.7 (258)	1077.8
Ar		−527.560002		
Xe		−15.539282		

[a] The experimentally observed frequencies are listed for comparison.

the Rh(η^2-O_2)$_2$(η^1-OO)(Ar) complex, and the 1252.9, 1129.2, and 1077.8 cm^{-1} absorptions to the Rh(η^2-O_2)$_2$(η^1-OO)(Xe) complex.

The assignment is strongly supported by DFT/B3LYP calculations. Geometric optimizations found a stable doublet Rh(η^2-O_2)$_2$(η^1-OO) structure with a C_s symmetry (Figure 7). Two O_2 subunits are side-on bonded and are equivalent; the third O_2 subunit is end-on bonded with the RhOO plane perpendicular to the $(O_2)_2$ plane. A stable quartet with very similar geometry is predicted to be only 0.8 kcal/mol less stable than the doublet. In addition, our theoretical calculations indicate that Rh(η^2-O_2)$_2$(η^1-OO) can coordinate one argon atom in forming the Rh(η^2-O_2)$_2$(η^1-OO)(Ar) complex. As shown in Figure 7, the Rh(η^2-O_2)$_2$(η^1-OO)(Ar) complex has a $^2A'$ ground state with a C_s symmetry. The Ar atom and the end-on bonded O_2 subunit are in the same plane. The three O−O stretching modes of the Rh(η^2-O_2)$_2$(η^1-OO)(Ar) complex were computed at 1390.6, 1240.5, and 1193.8 cm^{-1}, respectively, in good agreement with the observed values. When the Ar atom in Rh(η^2-O_2)$_2$(η^1-OO)(Ar) was replaced by Xe, the three O−O stretching vibrational modes were predicted to be 1350.5, 1243.9, and 1197.7 cm^{-1}, respectively. The end-on bonded O−O stretching mode red-shifted by 40.1 cm^{-1}, whereas the two stretching modes of the side-on bonded O_2 subunits blue-shifted by 3.4 and 3.9 cm^{-1} with respect to those of the Rh(η^2-O_2)$_2$(η^1-OO)(Ar) complex, which are also in quite reasonable agreement with the experimentally observed shifts of −27.2, 1.6, and 1.1 cm^{-1}.

Reaction Mechanism. The experimental observations clearly demonstrate that the ground-state rhodium atoms react with O_2 in argon to form the rhodium−dioxygen complexes, which are coordinated by one or two argon atoms, reactions 1−3:

$$\mathrm{Rh}\ (^4\mathrm{F}) + \mathrm{O_2}\ (^3\textstyle\sum_g^-) \rightarrow \mathrm{Rh}(\eta^2\text{-}\mathrm{O_2})\ (^2\mathrm{A_2}) \qquad \Delta E = -23.6\ \mathrm{kcal/mol}$$

$$\mathrm{Rh}(\eta^2\text{-}\mathrm{O_2})\ (^2\mathrm{A_2}) + 2\mathrm{Ar} \rightarrow \mathrm{Rh}(\eta^2\text{-}\mathrm{O_2})(\mathrm{Ar})_2\ (^2\mathrm{A_2}) \qquad \Delta E = -6.7\ \mathrm{kcal/mol} \quad (1)$$

$$\mathrm{Rh}(\eta^2\text{-}\mathrm{O_2})(\mathrm{Ar})_2\ (^2\mathrm{A_2}) + \mathrm{O_2}\ (^3\textstyle\sum_g^-) \rightarrow \mathrm{Rh}(\eta^2\text{-}\mathrm{O_2})_2(\mathrm{Ar})_2\ (^4\mathrm{B_{2u}}) \qquad \Delta E = -29.4\ \mathrm{kcal/mol} \quad (2)$$

$$\mathrm{Rh}(\eta^2\text{-}\mathrm{O_2})_2(\mathrm{Ar})_2\ (^4\mathrm{B_{2u}}) + \mathrm{O_2}\ (^3\textstyle\sum_g^-) \rightarrow \mathrm{Rh}(\eta^2\text{-}\mathrm{O_2})_2(\eta^1\text{-}\mathrm{OO})\ (\mathrm{Ar})\ (^2\mathrm{A'}) + \mathrm{Ar} \qquad \Delta E = -4.3\ \mathrm{kcal/mol} \quad (3)$$

Under visible light (λ > 500 nm) irradiation, the Rh(η^2-O_2)-(Ar)$_2$ absorption decreased, during which the RhO_2 absorptions increased. It appears that visible light initiates insertion reaction 4, which was predicted to be exothermic by about 35.4 kcal/mol.

$$Rh(\eta^2\text{-}O_2)\ (^2A_2) \rightarrow RhO_2\ (^2A_1) \qquad \Delta E = -35.4\ \text{kcal/mol} \quad (4)$$

In the experiments doping with xenon in argon, xenon atoms can readily replace argon atoms in the coordination sphere of the rhodium−dioxygen complexes. Consistent with this notion, the predicted binding energies of the Xe complexes are larger than those of the Ar complexes. The total binding energy of $Rh(\eta^2\text{-}O_2)(Ar)_2$ with respect to $Rh(\eta^2\text{-}O_2)$ and two Ar atoms is predicted to be 6.7 kcal/mol after zero-point energy and basis set superposition error corrections. This value increases to 10.6 kcal/mol when one Ar atom is replaced by Xe, and to 14.1 kcal/mol when both Ar atoms are replaced by xenon atoms. These binding energies are calculated with different basis sets on Ar and Xe. The calculated binding energies are about the same when the same basis set was used for Ar and Xe (SDD). The $Rh(\eta^2\text{-}O_2)_2(Ng)_2$ and $Rh(\eta^2\text{-}O_2)_2(\eta^1\text{-}OO)(Ng)$ (Ng = Ar, Xe) complexes are much weakly bound than the $Rh(\eta^2\text{-}O_2)(Ng)_2$ complex. As shown in Figure 7, the Rh−Ng bond distances of $Rh(\eta^2\text{-}O_2)_2(Ng)_2$ and $Rh(\eta^2\text{-}O_2)_2(\eta^1\text{-}OO)(Ng)$ are significantly longer than those of $Rh(\eta^2\text{-}O_2)(Ng)_2$.

Conclusions

The reaction of rhodium atoms and molecular oxygen was reinvestigated in solid argon. The reaction product absorptions are identified on the basis of isotopic substitution and density functional theoretical calculations at the B3LYP/aug-cc-PVTZ/SDD level of theory. The rhodium−dioxygen complexes $Rh(\eta^2\text{-}O_2)$, $Rh(\eta^2\text{-}O_2)_2$, and $Rh(\eta^2\text{-}O_2)_2(\eta^1\text{-}OO)$ are produced spontaneously on annealing. The $Rh(\eta^2\text{-}O_2)$ complex rearranges to the inserted RhO_2 molecule under visible light irradiation, indicating that the formation of dioxide requires activation energy. In addition, both experimental observations and theoretical calculation results indicate that the observed rhodium−dioxygen complexes are coordinated by one or two argon atoms in solid argon matrix and should be regarded as the $Rh(\eta^2\text{-}O_2)(Ar)_2$, $Rh(\eta^2\text{-}O_2)_2(Ar)_2$, and $Rh(\eta^2\text{-}O_2)_2(\eta^1\text{-}OO)(Ar)$ complexes instead of the isolated $Rh(\eta^2\text{-}O_2)$, $Rh(\eta^2\text{-}O_2)_2$, and $Rh(\eta^2\text{-}O_2)_2(\eta^1\text{-}OO)$ molecules. In the experiments with xenon doped in argon, the coordinated argon atoms can be readily replaced by xenon atoms to form the $Rh(\eta^2\text{-}O_2)(Ar)_{2-x}(Xe)_x$, $Rh(\eta^2\text{-}O_2)_2(Ar)_{2-x}(Xe)_x$ ($x = 1, 2$), and $Rh(\eta^2\text{-}O_2)_2(\eta^1\text{-}OO)(Xe)$ complexes.

Acknowledgment. We gratefully acknowledge financial support from the National Natural Science Foundation of China (Grant No. 20433080).

References and Notes

(1) See, for example: (a) Wayland, B. B.; Newman, A. R. *Inorg. Chem.* **1981**, *20*, 3093. (b) Jorgensen, K. A. *Chem. Rev.* **1989**, *89*, 431. (c) Ahijado, M.; Braun, T.; Noveski, D.; Kocher, N.; Neumann, B.; Stalke, D.; Stammler, H. G. *Angew. Chem., Int. Ed.* **2005**, *44*, 6947.

(2) Li, X.; Wang, L. S. *J. Chem. Phys.* **1998**, *109*, 5264.

(3) (a) Heuff, R. F.; Balfour, W. J.; Adam, A. G. *J. Mol. Spectrosc.* **2002**, *216*, 136. (b) Jensen, R. H.; Fougere, S. G.; Balfour, W. J. *Chem. Phys. Lett.* **2003**, *370*, 106. (c) Heuff, R. F.; Fougere, S. G.; Balfour, W. J. *J. Mol. Spectrosc.* **2005**, *231*, 99.

(4) (a) Mains, G. J.; White, J. M. *J. Phys. Chem.* **1991**, *95*, 112. (b) Siegbahm, P. E. M. *Chem. Phys. Lett.* **1993**, *201*, 15. (c) Stevens, F.; Van, Speybroeck, V.; Carmichael, I.; Callens, F.; Waroquier, M. *Chem. Phys. Lett.* **2006**, *421*, 281.

(5) Hanlan, A. J. L.; Ozin, G. A. *Inorg. Chem.* **1977**, *16*, 2848.

(6) Hanlan, A. J. L.; Ozin, G. A. *Inorg. Chem.* **1977**, *16*, 2857.

(7) Van, Zee, R. J.; Hamrick, Y. M.; Li, S.; Weltner, W., Jr. *J. Phys. Chem.* **1992**, *96*, 7247.

(8) Citra, A.; Andrews, L. *J. Phys. Chem. A* **1999**, *103*, 4845.

(9) (a) Chen, M. H.; Wang, X. F.; Zhang, L. N.; Yu, M.; Qin, Q. Z. *Chem. Phys.* **1999**, *242*, 81. (b) Zhou, M. F.; Andrews, L.; Bauschlicher, C W., Jr. *Chem. Rev.* **2001**, *101*, 1931.

(10) Frisch, M. J.; Trucks, G. W.; Schlegel, H. B.; Scuseria, G. E.; Robb, M. A.; Cheeseman, J. R.; Montgomery, J. A., Jr.; Vreven, T.; Kudin, K. N.; Burant, J. C.; Millam, J. M.; Iyengar, S. S.; Tomasi, J.; Barone, V.; Mennucci, B.; Cossi, M.; Scalmani, G.; Rega, N.; Petersson, G. A.; Nakatsuji, H.; Hada, M.; Ehara, M.; Toyota, K.; Fukuda, R.; Hasegawa, J.; Ishida, M.; Nakajima, T.; Honda, Y.; Kitao, O.; Nakai, H.; Klene, M.; Li, X.; Knox, J. E.; Hratchian, H. P.; Cross, J. B.; Adamo, C.; Jaramillo, J.; Gomperts, R.; Stratmann, R. E.; Yazyev, O.; Austin, A. J.; Cammi, R.; Pomelli, C.; Ochterski, J. W.; Ayala, P. Y.; Morokuma, K.; Voth, G. A.; Salvador, P.; Dannenberg, J. J.; Zakrzewski, V. G.; Dapprich, S.; Daniels, A. D.; Strain, M. C.; Farkas, O.; Malick, D. K.; Rabuck, A. D.; Raghavachari, K.; Foresman, J. B.; Ortiz, J. V.; Cui, Q.; Baboul, A. G.; Clifford, S.; Cioslowski, J.; Stefanov, B. B.; Liu, G.; Liashenko, A.; Piskorz, P.; Komaromi, I.; Martin, R. L.; Fox, D. J.; Keith, T.; Al-Laham, M. A.; Peng, C. Y.; Nanayakkara, A.; Challacombe, M.; Gill, P. M. W.; Johnson, B.; Chen, W.; Wong, M. W.; Gonzalez, C.; Pople, J. A. *Gaussian 03*, revision B.05; Gaussian, Inc.: Pittsburgh, PA, 2003.

(11) Becke, A. D. *J. Chem. Phys.* **1993**, *98*, 5648.

(12) Lee, C.; Yang, W.; Parr, R. G. *Phys. Rev. B* **1988**, *37*, 785.

(13) (a) Dunning, T. H., Jr. *J. Chem. Phys.* **1989**, *90*, 1007. (b) Kendall, R. A.; Dunning, T. H., Jr.; Harrison, R. J. *J. Chem. Phys.* **1992**, *96*, 6769.

(14) (a) Dolg, M.; Stoll, H.; Preuss, H. *J. Chem. Phys.* **1989**, *90*, 1730. (b) Andrae, D.; Haussermann, U.; Dolg, M.; Stoll, H.; Preuss, H. *Theor. Chim. Acta* **1990**, *77*, 123.

(15) Chertihin, G. V.; Andrews, L. *J. Chem. Phys.* **1998**, *108*, 6404.

(16) Li, J.; Bursten, B. E.; Liang, B.; Andrews, L. *Science* **2002**, *295*, 2242.

(17) (a) Andrews, L.; Liang, B. Y.; Li, J.; Bursten, B. E. *J. Am. Chem. Soc.* **2003**, *125*, 3126. (b) Andrews, L.; Liang, B. Y.; Li, J.; Bursten, B. E. *Angew. Chem., Int. Ed.* **2000**, *39*, 4565.

(18) Li, J.; Bursten, B. E.; Andrews, L.; Marsden, C. J. *J. Am. Chem. Soc.* **2004**, *126*, 3424.

(19) Wang, X. F.; Andrews, L.; Li, J.; Bursten, B. E. *Angew. Chem., Int. Ed.* **2004**, *43*, 2554.

(20) (a) Zhao, Y. Y.; Wang, G. J.; Chen, M. H.; Zhou, M. F. *J. Phys. Chem. A* **2005**, *109*, 6621. (b) Zhao, Y. Y.; Gong, Y.; Chen, M. H.; Ding, C. F.; Zhou, M. F. *J. Phys. Chem. A* **2005**, *109*, 11765.

(21) Zhao, Y. Y.; Gong, Y.; Chen, M. H.; Zhou, M. F. *J. Phys. Chem. A* **2006**, *110*, 1845.

(22) Zhao, Y. Y.; Gong, Y.; Zhou, M. F. *J. Phys. Chem. A* **2006**, *110*, 10777.

(23) Ono, Y.; Taketsugu, T. *Chem. Phys. Lett.* **2004**, *385*, 85.